

Synthesis of high-surface-area ruthenium oxide aerogels by non-alkoxide sol–gel route

Dong Jin Suh^{a,*}, Tae-Jin Park^a, Won-Il Kim^b, In-Kwon Hong^b

^a*Clean Technology Research Center, Korea Institute of Science and Technology,
P.O. Box 131, Cheongryang, Seoul 136-791, South Korea*

^b*Department of Chemical Engineering, Dankook University, San 8, Hannam-dong,
Yongsan-gu, Seoul 140-714, South Korea*

Received 23 August 2002; accepted 9 November 2002

Abstract

High-surface-area ruthenium oxide aerogels with pronounced mesoporosity are prepared by carbon dioxide supercritical drying of alcogels by a non-alkoxide sol–gel process with ruthenium chloride as a precursor and epoxide as a proton scavenger. The influence of various sol–gel preparation parameters both on gel formation and the textural properties and voltammetric response of the resulting ruthenium oxide aerogels are investigated systematically. The un-calcined ruthenium oxide aerogel in the amorphous phase possesses a surface area in excess of $350 \text{ m}^2 \text{ g}^{-1}$ has a specific capacitance as high as 595 F g^{-1} .

© 2002 Elsevier Science B.V. All rights reserved.

Keywords: Ruthenium oxide; Sol–gel; Aerogel; Surface area; Specific capacitance

1. Introduction

Ruthenium oxide is presently of great interest in a wide range of electrocatalytic applications including electrolytic production of chlorine gas from brine [1,2]. It is also a major component of the Pt–Ru anode catalysts used for direct methanol fuel cells [3]. In particular, ruthenium oxide and its hydrates have been studied as high energy-storage electrode materials because of their high capacitance and low resistance. Conway [4] has reported that ruthenium oxides with a high surface-area are promising electrode materials for electrochemical capacitors. Zheng and Jow [5] have also demonstrated the high-energy storage characteristics of the amorphous form of hydrous ruthenium oxides prepared by a sol–gel process at low temperatures.

For electrocatalytic as well as capacitive applications, it is desirable to maximize the specific surface-area of ruthenium oxide. Ruthenium oxide samples prepared by the conventional thermal decomposition of chloride precursor materials have very low surface-areas and a crystalline phase [6]. Although several liquid-phase preparation procedures have been applied to obtain high-surface-area ruthenium oxides, the highest reported specific surface-area is about $120 \text{ m}^2 \text{ g}^{-1}$ [7].

The sol–gel to aerogel route can be an efficient method to prepare high-surface-area metal oxide forms. Aerogels are a class of nanostructured materials with high porosity, low density, and high surface-area. Aerogels are prepared by sol–gel synthesis and subsequent supercritical drying to avoid collapse of the original gel structure due to surface tension. Generally, the sol–gel method uses metal alkoxides as precursors because of their high sol–gel reactivity. Most of the metal alkoxides, however, are very expensive and sometimes not commercially available. In addition, it is not easy to handle them due to their high sensitivity to heat, moisture, and light. Meanwhile, Itoh et al. [8] have reported the use of propylene oxide in the sol–gel preparation of silicate–aluminate gels using hydrated aluminum chloride as the aluminum oxide source. Tillotson et al. [9] also used propylene oxide as a gelation promoter in the sol–gel synthesis of lanthanide and lanthanide–silicate gels using hydrated lanthanide nitrate salts [9]. More recently, a new sol–gel method using simple inorganic salt precursors has been developed by researchers at Lawrence Livermore National Laboratory [10,11]. Iron oxide and chromia aerogels have been prepared by this method. The success of this synthetic route may be due to the use of epoxides as gelation agents for the sol–gel synthesis.

In this work, an attempt is made to find the optimum conditions to synthesize high-surface-area ruthenium oxide

* Corresponding author. Tel.: +82-2-958-5192; fax: +82-2-958-5199.
E-mail address: djsuh@kist.re.kr (D.J. Suh).

aerogels through the non-alkoxide sol–gel route. A systematic investigation is under taken of the influence of various preparation parameters on the textural properties and voltammetric response of the ruthenium oxide aerogels.

2. Experimental

Ruthenium chloride hydrate, $\text{RuCl}_3 \cdot x\text{H}_2\text{O}$ (99.9%), as a metal precursor and propylene oxide (99%) and 1,2-epoxybutane (99%) as gelation agents were obtained from Aldrich and used as received. Methanol and ethanol (Merck) were used as solvents for liquid chromatography and were reagent grade. All syntheses were performed under ambient conditions. $\text{RuCl}_3 \cdot x\text{H}_2\text{O}$ was first dissolved in methanol or ethanol and distilled water was added to the solution. The desired amount of epoxide, propylene oxide or 1,2-epoxybutane, was quickly added to the solution under vigorous stirring. Stirring was continued until the vortex created by the stirring disappeared. The time required for this to happen was defined as the gel time. The wet gel was then covered with plastic film and allowed to age for a few days at room temperature. The alcohol solvent was removed from the wet gels by contact with flowing supercritical carbon dioxide at 333 K and 11 MPa. The resulting aerogels were ground to pass a 100 mesh screen and finally calcined in flowing helium at different temperatures. Cryogel and xerogel samples were prepared for comparison and came from the same gel and differed only in the drying methods, i.e. freeze and conventional drying.

After supercritical drying and calcination, textural characterization of the aerogel samples was performed on a Micromeritics ASAP 2010 surface-area analyzer. The BET surface-area, pore volume, and pore-size distribution were obtained by nitrogen adsorption–desorption at 77 K. The mesopore size distributions were calculated by applying the Barrett–Joyner–Halenda method to the desorption branch of the isotherm [12]. Prior to the measurements, all samples were outgassed at 393 K overnight. Crystalline structures were determined by X-ray diffraction (XRD) experiments performed on a Rigaku D/MAX-II A diffractometer using $\text{Cu K}\alpha$ radiation.

Specific capacitances of selected aerogel samples were determined by cyclic voltammetry (CV) measurements in 0.5 M H_2SO_4 . Electrochemical measurements were performed using a EG&G Model 273A potentiostat/galvanostat connected to a conventional three-compartment cell which comprised a ruthenium oxide aerogel working electrode, a platinum foil counter electrode, and a saturated calomel reference electrode (SCE). The electrolyte was thoroughly purged with nitrogen prior to and during measurements. The preparation of thin-film electrodes followed the method described by Schmidt et al. [13]. Ruthenium oxide aerogel (20 mg) was dispersed ultrasonically in 2 ml distilled water for 2 h. Then a 20 μl aliquot was transferred on to a polished carbon substrate (5.4 mm diameter, 0.229 cm^2) to yield an

electrocatalyst loading of 870 $\mu\text{g cm}^{-2}$. After drying at 60 $^\circ\text{C}$, 20 μl of a 5 wt.% Nafion alcoholic solution (Aldrich) was further dropped on the resulting thin-film electrode surface in order to fix the electrocatalyst to the carbon substrate rod.

3. Results and discussion

3.1. Gel formation

The effects of the water and epoxide contents on gel time are illustrated in Figs. 1 and 2, respectively. The notations represent the solvents and epoxides that were used, namely: E, ethanol; M, methanol; P, propylene oxide; B, 1,2-epoxybutane. In Fig. 1, the contents of solvents and epoxides are fixed at 30 and 10 mol mol^{-1} of ruthenium precursor, respectively. The gel time was observed to increase as the water content increased. The gel obtained was hard when the water content was in the range of 30–120 mol mol^{-1} Ru, but became soft with a higher water content of 120–200 mol mol^{-1} Ru. When the water content was over 200 mol mol^{-1} Ru, the gel was not formed probably because the precursor concentration was too low. On the other hand, a gelatinous precipitate was obtained with a water content of lower than 30 mol mol^{-1} Ru, probably because the hydrolysis reaction could not proceed well.

Gels were made by adding a sufficient amount of water to complete the hydrolysis reaction under not quite dilute conditions. The gel time for ruthenium oxide wet gel appeared to be dependent on the type of the solvent. The gel time was shorter when ethanol as opposed to methanol was used as a solvent. This may be due to the difference in solubility of the ruthenium oxide sol particles in each

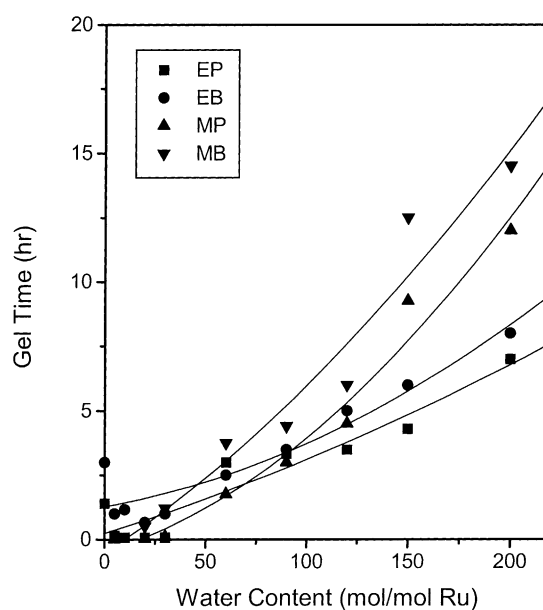


Fig. 1. Effect of water content on gel time: E, ethanol; M, methanol; P, propylene oxide; B, 1,2-epoxybutane.

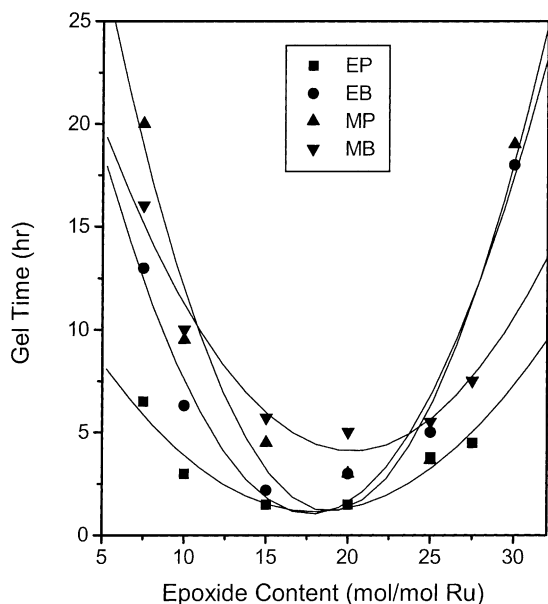


Fig. 2. Effect of epoxide content on gel time: E, ethanol; M, methanol; P, propylene oxide; B, 1,2-epoxybutane.

solvent [10]. The gel time was also dependent on the type of epoxide. The gel time was longer with 1,2-epoxybutane than with propylene oxide, probably because the former with a bulkier molecular structure has a lower protonation rate.

As shown in Fig. 2, an optimum range of epoxide/Ru ratio for the rate of gel formation was observed regardless of the types of epoxide and solvent. The gels produced with an epoxide content of 10–15 mol mol⁻¹ precursor appeared to be hard, while those with the higher content of 15–25 were soft. Gels were not produced with an epoxide content of <5 mol mol⁻¹ precursor because the amount of epoxide, which served as a proton scavenger, was not sufficient for the gelation to proceed. The nucleophiles present in the solution were Cl⁻ and H₂O. The better nucleophile, Cl⁻ preferentially attacked a ring carbon of the protonated epoxide to

given rise to the formation of chloropropanol by ring opening. This caused the gradual consumption of protons from solution and, consequently, the formation of an aquo-hydroxy species of Ru³⁺. The latter, in turn, underwent further hydrolysis and condensation to form a polymeric gel. On the other hand, H₂O could be competitive with Cl⁻ for ring opening of the protonated epoxide, which induced an undesirable deprotonation reaction to give 1,2-propanediol. Therefore, the required amounts of water and epoxide are higher than the stoichiometric values [11].

3.2. Textural properties

The textural properties of ruthenium oxide aerogels prepared under different conditions are listed in Tables 1 and 2. The aerogels have specific surface-areas that range from 20 to 378 m² g⁻¹, and average pore diameters in the mesopore range of 2–30 nm. As shown in Table 1, the specific surface-area is higher with ethanol and propylene oxide than with methanol and 1,2-epoxybutane. The maximum surface-area of 378 m² g⁻¹ is obtained with 60 mol of water per mol of precursor for the ethanol–propylene oxide combination. As shown in Fig. 3, the aerogel has pronounced mesoporosity in the range 10–100 nm with a narrow pore-size distribution. Gelatinous precipitates prepared at lower water content of <30 mol mol⁻¹ Ru lead to relatively lower specific surface-areas and pore volumes with broader pore-size distributions. Similar behavior is encountered for soft gels prepared at a high water content of more than 120 mol mol⁻¹, possibly due to some collapse of the initial gel framework during the supercritical drying step. In fact, collapse and shrinkage are likely to occur with sol–gel products that contain high water content because the water existing inside the porous structure of the gel cannot reach the supercritical state.

The textural properties of the aerogels are also dependent on the epoxide content, as shown in Table 2. The specific surface-area is higher than 250 m² g⁻¹ with an epoxide

Table 1

Effect of water content on textural properties of resulting ruthenium oxide aerogels after supercritical drying: E, ethanol; M, methanol; P, propylene oxide; B, 1,2-epoxybutane

Water content ^a	EP			EB			MP			MB		
	<i>S</i> _{BET} ^b	<i>V</i> _P ^c	<i>D</i> _P ^d	<i>S</i> _{BET} ^b	<i>V</i> _P ^c	<i>D</i> _P ^d	<i>S</i> _{BET} ^b	<i>V</i> _P ^c	<i>D</i> _P ^d	<i>S</i> _{BET} ^b	<i>V</i> _P ^c	<i>D</i> _P ^d
5	322	0.58	7.1	143	0.37	10.4	20	0.02	4.0	98	0.06	2.4
10	321	0.62	7.8	145	0.39	10.7	95	0.06	2.6	106	0.12	4.4
20	209	0.46	8.8	279	0.54	7.7	210	0.39	7.6	104	0.28	10.8
30	343	0.73	8.5	237	0.52	8.9	274	0.50	7.3	119	0.45	15.1
60	378	2.04	21.5	359	2.23	24.8	297	1.59	21.3	273	1.14	16.7
90	291	1.64	22.5	290	1.06	14.6	105	0.45	17.3	85	0.21	10.0
120	227	0.73	12.9	135	0.18	5.3				57	0.03	2.0
150	143	0.09	2.5	47	0.14	11.8						

^a Water content (mol mol⁻¹ Ru) used in sol–gel process.

^b BET surface-area (m² g⁻¹).

^c Total pore volume (cm³ g⁻¹).

^d Average pore diameter (nm) calculated from 4 × *S*_{BET}/*V*_P.

Table 2

Effect of epoxide content on textural properties of resulting ruthenium oxide aerogels after supercritical drying: E, ethanol; M, methanol; P, propylene oxide; B, 1,2-epoxybutane

Epoxide content ^a	EP			EB			MP			MB		
	$S_{\text{BET}}^{\text{b}}$	V_{P}^{c}	D_{P}^{d}	$S_{\text{BET}}^{\text{b}}$	V_{P}^{c}	D_{P}^{d}	$S_{\text{BET}}^{\text{b}}$	V_{P}^{c}	D_{P}^{d}	$S_{\text{BET}}^{\text{b}}$	V_{P}^{c}	D_{P}^{d}
10	378	2.04	21.5	359	2.23	24.8	283	1.54	21.8	273	1.14	16.7
15	345	0.73	8.4	287	1.90	26.4	275	1.03	14.9	308	1.73	22.5
20	327	0.59	7.2	246	0.79	12.9				236	1.25	21.1
25	182	0.24	5.4	38	0.06	6.7				213	0.50	9.4

^a Epoxide content (mol mol^{-1} Ru) used in sol–gel process.

^b BET surface-area ($\text{m}^2 \text{g}^{-1}$).

^c Total pore volume ($\text{cm}^3 \text{g}^{-1}$).

^d Average pore diameter (nm) calculated from $4 \times S_{\text{BET}}/V_{\text{P}}$.

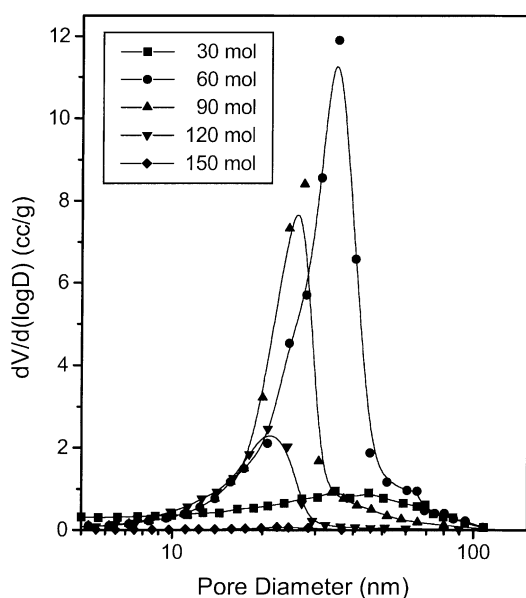


Fig. 3. Pore-size distribution of resulting ruthenium oxide aerogels as a function of water content used in sol–gel synthesis.

content of 10–15 mol mol^{-1} precursor, and decreases on increasing the amount of epoxide to produce weakly-branched soft gels. As a result, clear and hard gels, which are obtained with shorter gel time, exhibit higher specific surface-areas and pore volumes with the narrow pore-size distribution of the corresponding aerogels. This is probably due to the inherent rigid porous network structure of the polymeric gels.

3.3. Calcination

The textural properties of the aerogel, cryogel, and xerogel samples calcined at a range of temperatures are given in Table 3. As regards texture, the aerogel possesses a high surface-area of $378 \text{ m}^2 \text{g}^{-1}$ and is mesoporous, whereas the corresponding cryogel and xerogel, which come from the same wet gel and differ only in the drying method, have lower surface areas of 213 and $14 \text{ m}^2 \text{g}^{-1}$, respectively, with a prominent contribution of microporosity. For all the sample, both the surface-area and the pore volume decrease as the calcination temperature is increased. As shown in Fig. 4, the pore-size distribution of the aerogel sample

Table 3

Textural properties of ruthenium oxide aerogel, cryogel, and xerogel calcined at different temperatures under helium flow

Temperature ^a	Aerogel			Cryogel			Xerogel		
	$S_{\text{BET}}^{\text{b}}$	V_{P}^{c}	D_{P}^{d}	$S_{\text{BET}}^{\text{b}}$	V_{P}^{c}	D_{P}^{d}	$S_{\text{BET}}^{\text{b}}$	V_{P}^{c}	D_{P}^{d}
After drying	378	2.04	21.5	213	0.10	2.0	14	0.008	1.8
423	307	1.42	18.5	1.8	0.002	6.0	0.05	–	–
443	302	1.49	19.7	1.0	0.001	0.1	0.05	–	–
473	251	1.30	20.7						
523	153	0.70	18.3						
573	146	0.75	20.7						
673	110	0.65	23.6						
773	50	0.26	21.1						

^a Calcination temperature (K).

^b BET surface area ($\text{m}^2 \text{g}^{-1}$).

^c Total pore volume ($\text{cm}^3 \text{g}^{-1}$).

^d Average pore diameter (nm) calculated from $4 \times S_{\text{BET}}/V_{\text{P}}$.

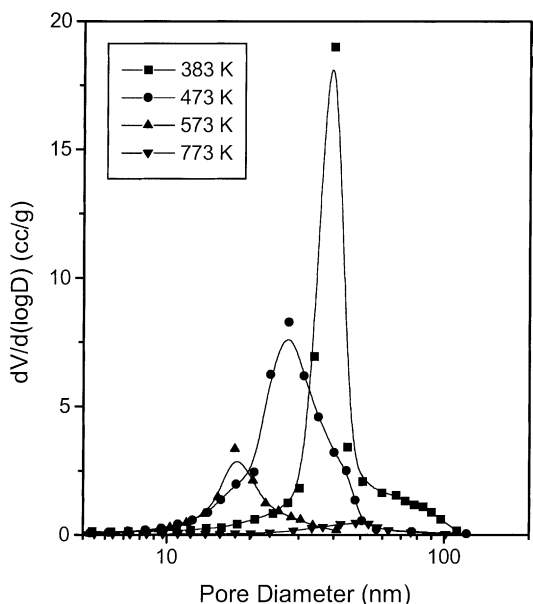


Fig. 4. Pore-size distribution of the ruthenium oxide aerogels calcined at different temperatures under helium flow.

broadens and its maximum shifts to smaller pore diameters on increasing the calcination temperature. Heat treatment up to 473 K do not radically change the textural characteristics of the calcined ruthenium oxide aerogel. By contrast, the surface-area and the pore volume decrease significantly after calcination at 523 K without apparent change in average pore diameter. On the other hand, since the cryogel and xerogel have relatively poor thermal stability, the corresponding surface-area and pore volume decrease dramatically to 1.8 and 0.05 m² g⁻¹, respectively, after calcination at 423 K.

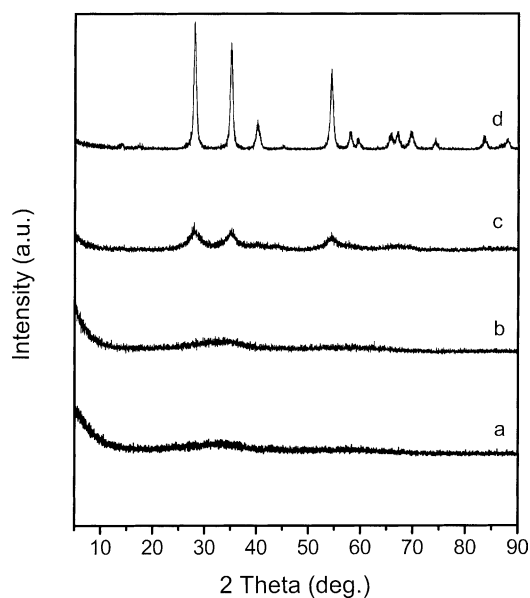


Fig. 5. X-ray diffraction patterns for ruthenium oxide aerogels calcined at different temperatures under helium flow: (a) after supercritical drying; (b) 473 K; (c) 573 K; (d) 773 K.

The crystalline structure of the aerogel has been studied as a function of the calcination temperature. From the X-ray diffraction results shown in Fig. 5, it is found that the aerogels remain X-ray amorphous up to 473 K. Calcination at 573 K results in crystallite formation into the rutile phase of anhydrous RuO₂, despite the fact that broad and weak X-ray diffraction peaks indicate poor crystallinity. This crystalline transition, an exothermic phenomenon which is detected by TG-DTA (thermogravimetric and differential thermal analysis) techniques, may cause a considerable loss in the surface-area of the aerogel sample after calcination at 523 K.

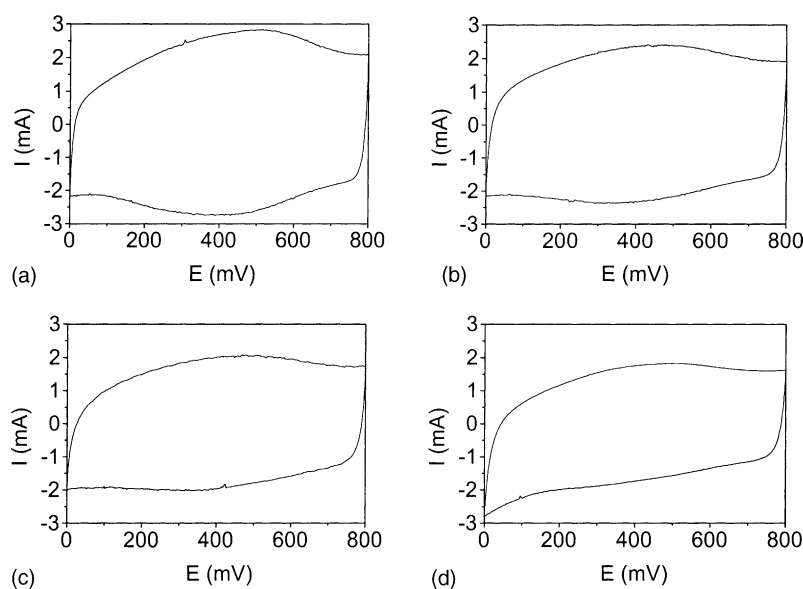


Fig. 6. Cyclic voltammograms (0.5 M H₂SO₄; at 20 mV s⁻¹) of ruthenium oxide aerogels calcined at different temperatures: (a) after supercritical drying; (b) 423 K; (c) 443 K; (d) 473 K.

Table 4
Specific capacitance of ruthenium oxide aerogels calcined at different temperatures under helium flow

Temperature (K)	Specific capacitance (F g ⁻¹)	Capacitance/BET area (F m ⁻²)
– ^a	595	1.57
423	525	1.71
443	443	1.47
473	394	1.57
523	179	1.16
573	106	0.73
773	21	0.42

^a After supercritical drying.

Further calcination at higher temperatures leads to the growth of the rutile phase RuO₂ crystalline particles.

3.4. Specific capacitance

Cyclic voltammetric (CV) curves of ruthenium oxide aerogel electrodes calcined at different temperatures are shown in Fig. 6. The curves were obtained in 0.5 M H₂SO₄ at a potential sweep rate of 20 mV s⁻¹. The CV curves are similar to those of ruthenium oxide electrodes presented elsewhere [6], and indicate capacitive behavior. Capacitance measurements are derived from the respective voltammograms: $C = i/s$, where i and s are the current response and the potential sweep rate (dV/dt), respectively. The specific capacitances are averaged by measuring the current from 0.2 to 0.7 V in the voltammetric sweep [14], and are listed in Table 4.

Amorphous ruthenium oxide aerogels calcined at relatively low temperatures are found to have high specific capacitances. When the crystalline phase is formed after calcination at 523 K, the specific capacitance drops significantly. The highest specific capacitance of 595 F g⁻¹ obtained for the uncalcined aerogel. The capacitance is almost proportional to the surface-area of the ruthenium oxide electrode material provided the material exists in the amorphous state. The specific capacitances of ruthenium oxides are known to depend on the degree of hydration and crystallinity [5,6]. High surface-area ruthenium oxide aerogels, if prepared in the form of amorphous hydrous oxides by further controlling the heat-treatment conditions, may exhibit much higher specific capacitances. In practice, the real surface-area estimated by gas adsorption may differ significantly from the electrochemically active surface available for charged species. As discussed earlier, however, since ruthenium oxide aerogels are not microporous but mostly mesoporous, their porous network structure is likely to be voltammetrically accessible in liquid electrolyte.

4. Conclusions

High-surface-area ruthenium oxide aerogels are prepared by the sol–gel process with propylene oxide and ruthenium chloride and subsequent carbon dioxide supercritical drying. Epoxide may act as an irreversible proton scavenger to induce polymeric ruthenium oxide gels. The maximum surface area of 378 m² g⁻¹ is obtained with 60, 30, and 10 mol of water, ethanol, and propylene oxide per unit mol of ruthenium, respectively. Clear and hard gels, which are obtained with shorter gel times, exhibit higher surface-areas and pore volumes with the narrow pore-size distributions of the corresponding aerogels. This is probably due to the inherent rigid porous network structure of the polymeric gels. The surface area and pore volume decrease as the calcination temperature is increase and decrease significantly after calcination at 523 K. This is probably due to crystallite formation into the rutile phase of anhydrous RuO₂. Amorphous ruthenium oxide aerogels calcined at lower temperatures are found to have high specific capacitances. When the crystalline phase is formed after calcination at 523 K, the specific capacitance drops significantly. The highest specific capacitance of 595 F s⁻¹ is obtained for the uncalcined aerogel.

References

- [1] B. Cornell, D. Simonsson, J. Electrochem. Soc. 140 (1993) 3123.
- [2] S. Trasatti, Electrochim. Acta 36 (1991) 225.
- [3] A. Hamnett, S.A. Weeks, B.J. Kennedy, G. Troughton, P.A. Christensen, Ber. Bunsenges Phys. Chem. 94 (1990) 1014.
- [4] B.E. Conway, J. Electrochem. Soc. 38 (1991) 1539.
- [5] J.P. Zheng, T.R. Jow, J. Electrochem. Soc. 142 (1995) L6.
- [6] J.P. Zheng, P.J. Cygan, T.R. Jow, J. Electrochem. Soc. 142 (1995) 2699.
- [7] I.D. Raistrick, R.T. Sherman, in: S. Srinivasan, S. Wagner, H. Wroblowa (Eds.), Proceedings of the 2nd Symposium on Electrode Materials and Processes for Energy Conversion and Storage, The Electrochemical Society Proceedings Series, Pennington, NJ, 1987, p. 582.
- [8] H. Itoh, T. Tabata, M. Kokitsu, N. Okazaki, Y. Imizu, A. Tada, J. Ceram. Soc. Jpn. 101 (1993) 1081.
- [9] T.M. Tillotson, W.E. Sunderland, I.M. Thomas, L.W. Hrubesh, J. Sol–Gel Sci. Technol. 1 (1994) 241.
- [10] A.E. Gash, T.M. Tillotson, J.H. Satcher Jr., L.W. Hrubesh, R.L. Simpson, J. Non-Cryst. Solids 285 (2001) 22.
- [11] A.E. Gash, T.M. Tillotson, J.H. Satcher Jr., J.F. Poco, L.W. Hrubesh, R.L. Simpson, Chem. Mater. 113 (3) (2001) 999.
- [12] E.P. Barrett, L.G. Joyner, P.P. Halenda, J. Am. Chem. Soc. 73 (1951) 373.
- [13] T.J. Schmidt, M. Noeske, H.A. Gasteiger, R.J. Behm, P. Britz, H. Bonemann, J. Electrochem. Soc. 145 (1998) 925.
- [14] J.W. Long, K.E. Swider, C.I. Merzbacher, D.R. Rolison, Langmuir 15 (3) (1999) 780.